Behaviour of fibre reinforced polymer-strengthened T-beams and slabs in fire

Adelzadeh, Masoud; Green, Mark F.; Bénichou, Noureddine

Publisher's version / Version de l'éditeur:
https://doi.org/10.1680/stbu.11.00014
Proceedings of the Institution of Civil Engineers: Structures and Buildings, 165, 7, pp. 361-371, 2012

NRC Publications Record / Notice d'Archives des publications de CNRC:
https://nrc-publications.canada.ca/eng/view/object/?id=309a4977-ef9e-4a18-873f-de2653e53388
https://publications-cnrc.canada.ca/fra/voir/objet/?id=309a4977-ef9e-4a18-873f-de2653e53388

Title: Behaviour in fire of FRP strengthened T-beams and slabs

Authors:
Masoud Adelzadeh, MSc
PhD Student, Civil Engineering Department, Queen's University
masoud.adelzadeh@ce.queensu.ca

Mark F. Green, PhD, PEng (corresponding author)
Professor, Civil Engineering Department, Queen's University,
58 University Ave., Kingston, ON K7L 3N6 Canada
greenm@civil.queensu.ca
Tel. 1 613 533-2147 Fax. 1 613 533-2128

Noureddine Bénichou, MASc, PhD
Senior Research Officer, Fire Resistance and Risk Management
NRC Institute for Research in Construction
1200 Montreal Road
Building M-59, Room 220
Ottawa, Ontario K1A 0R6
Noureddine.Benichou@nrc-cnrc.gc.ca

Number of words: 3,500

Number of figures: 11

Number of tables: 4

Abstract

This paper presents experimental and numerical results of intermediate-scale and full-scale fire tests conducted on flexurally strengthened reinforced concrete members. Two full-scale reinforced concrete T-beams and two intermediate-scale slabs were strengthened in flexure with carbon fibre reinforced polymer (CFRP) sheets or plates and insulated with a layer of spray-on material. T-beams and slabs were then exposed to a standard fire. T-beams were loaded to their service load. Deflections, strains, and temperatures were measured during the tests. A numerical finite difference/volume heat transfer model was used to simulate the temperature field inside the section. The validity of the numerical model was verified by comparing the predicted temperatures with those recorded during the fire test. Fire test results show that fire endurances of more than 4 hours can be achieved using the appropriate insulation system.

Notations:

c – heat capacity
CFRP – carbon fibre reinforced polymer
FOS – fibre optic sensor
FRP – fibre reinforced polymer
i – counter for time increments for finite difference
k – thermal conductivity
p – point in finite difference discretisation
t – time
T – temperature
T_g – glass transition temperature
x, y – spatial coordinates
ρ – density

Keywords: fire engineering, concrete structures, rehabilitation

1. INTRODUCTION

Fibre reinforced polymers (FRPs) have been commonly used in the aerospace and automotive industries. Recently, FRPs have gained popularity in the construction industry mainly due to ease of application, high strength and durability against corrosion.

FRP has been most often applied for strengthening of bridge structures where the risk of exposure to fire is comparably low. For building structures, where fire endurance is a primary design consideration, the lack of knowledge about fire performance limits the application of FRPs. To fulfill design requirements, one needs to know the behaviour of the material and structure at elevated temperatures. A measure of fire endurance commonly used by codes is the duration of fire exposure for a structural element before its failure. This time allows for safe evacuation of the building when a fire incident happens. The behaviour of steel and concrete at elevated temperatures is well-known (Lie, 1992, Buchanan, 2001, Purkiss, 2007, Bazant and Kaplan, 1996). This allows fairly accurate fire endurance calculations for reinforced concrete structures. On the contrary, limited data exist on the behaviour of FRP materials used as construction materials. Experimental results on the behaviour of FRP materials at elevated temperatures show a significant loss of mechanical properties at temperatures close to glass transition temperature (T_g) of the bonding resin (Chowdhury et al., 2010). At this temperature, the resin softens and the resin will no longer be as effective in transferring stresses between fibres and between the fibres and concrete. For most of the commercially available FRP materials for repair, T_g is usually between 50 and 100 °C. Fire exposed members will reach this temperature very rapidly in a post flashover fire situation; therefore FRP needs to be protected from direct fire exposure.

Only limited studies are available in the literature concerning the fire behaviour of externally FRP-strengthened members. Deuring (1994) tested six beams (300 mm × 400 mm × 5 m) where four of them were strengthened with CFRP sheets and were subjected to sustained loading. Insulated beams showed satisfactory fire endurance in the tests. The un-insulated beams had a fire endurance of 81 minutes while the insulated beams had an endurance of 146 minutes. Interestingly, the endurance of the insulated CFRP plated beam was longer than that of the un-strengthened reinforced concrete beam. Blontrock et al. (2000) tested CFRP plated beams using multiple insulation schemes. During the experiments, when the temperature of FRP reached T_g, the load bearing contribution of FRP was significantly reduced. Overall, the fire endurance observed in the tests was not sufficient for building performance. Other tests reported on full-scale insulated T-beams and slabs (Williams et al., 2008) found that the members could achieve up to 4 hours of fire endurance in the tests.

In this study, two full-scale reinforced concrete T-beams and two intermediate-scale slabs were strengthened in flexure with carbon fibre reinforced polymer (CFRP) sheets or plates and insulated with a layer of spray-on material. T-beams and slabs were then exposed to a standard fire. T-beams were loaded to their service load during fire endurance tests. As an extension of the work presented by Williams et al. (2008), the current study examines two different FRP materials and a different insulation system.

2. THE EXPERIMENTAL PROGRAM

The experimental program consisted of fire tests on two intermediate-scale reinforced concrete slabs and two full-scale reinforced concrete T-beams, all of which were strengthened with FRP materials applied externally to the specimens. The slabs were designated as slab-A and slab-B and

the T-beams were designated as beam-A and beam-B. The slabs were rectangular in shape, 1330 mm by 955 mm and 150 mm thick. Three 15 mm diameter deformed steel rebars were placed in the longer direction and three 10 mm diameter steel rebars were placed in the other direction at the bottom of the slabs. A clear concrete cover of 40 mm was provided for the steel rebars.

The T-beams had a span of 3.9 m and an overall height of 400 mm. The flange was 1220 mm wide and 150 mm thick while the web was 300 mm wide. The reinforcement details are shown in Figure 1. Two 15 mm diameter steel bars act as flexural internal reinforcement at the bottom of the beams. Clear concrete cover was 40 mm for both beams. The average measured yield stress of the steel was 470 MPa and the average measured 28 day compressive strength of the concrete was 32 MPa.

The slabs and T-beams were fabricated and cured indoors for at least six months at Queen's University and then shipped to the National Research Council for fire testing.

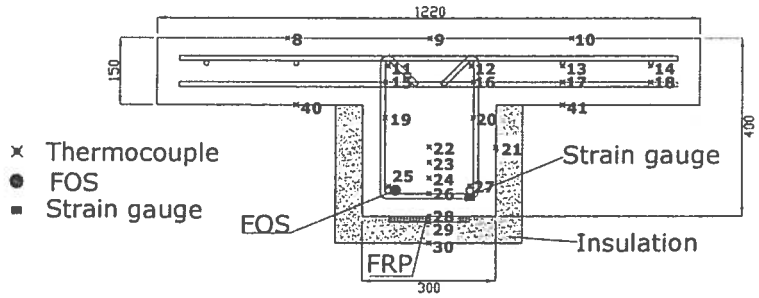

Figure 1. Details of reinforcement and instrumentation for beams (dimensions in mm).

3. Strengthening and Insulation

Either CFRP plates or CFRP sheets were installed on slab-A and slab-B respectively as shown in Table 2. One of the T-beams was strengthened by CFRP plates in flexure and the other was strengthened in flexure by 1 layer of CFRP sheets on the bottom of the web of the beam. Appropriate U-wrap was provided at the ends of the plates according to the provisions of ACI (2008). A summary of the strengthening system for T-beams is presented in Table 2. Table 3 gives a summary of the material properties of the FRP as provided by the manufacturer.

In order to provide supplemental fire insulation over the FRP on beams and slabs, a cement-based, dry mix fire protection mortar was applied as insulation. A 40 mm layer of insulation was spray-applied to slab-A, beam-A and beam-B, while the insulation thickness for slab-B was 60mm.

Table 1. FRP and insulation details for intermediate-scale slabs.

		slab A	slab B
FRP	Type	Sika CarboDur® S512	SikaWrap® Hex 103C
	No. Layers/strips	3 side by side	2
	FRP Width (mm)	3×50	635
Epoxy		SikaDur®-30	SikaDur®-300
Insulation	Type	Sikacrete®-213F	Sikacrete®-213F
	Insulation Thickness	40 mm	60 mm

Table 2. Summary of FRP-Insulation system used for T-beams.

		beam A	beam B
Flexural FRP	Type	Sika CarboDur® S812	SikaWrap® Hex 103C
	No. Layers/strips	1	1
	FRP Width (mm)	80	200
Insulation	Type	Sikacrete®-213F	
	Insulation Thickness	40 mm	
U-wrap END I	Type	SikaWrap® Hex 103C	SikaWrap® Hex 100G
	No. Layers	2	2
	Wrap Width (mm)	635	610
U-wrap ENDJ	Type	SikaWrap® Hex 230C	SikaWrap® Hex 430G
	No. Layers	4	4
	Wrap Width (mm)	600	610

Table 3. Material properties of FRP (provided by the manufacturer).

Material Type	Thickness (mm)	Modulus (Gpa)	Strength (Mpa)	Ultimate Strain(%)	Tg (C)
Sika CarboDur® S812 CFRP plate	1.20	165	2800	1.70	150
SikaWrap® Hex 103C CFRP sheet	1.02	70.6	849	1.12	-
SikaWrap® Hex 230C CFRP sheet	0.38	65.4	894	1.37	-
SikaWrap® Hex 100G GFRP sheet	1.02	26.1	612	2.34	-
SikaWrap® Hex 430G GFRP sheet	0.51	26.4	537	2.03	-
Sikadur 30 epoxy	-	4.5	24.8	1.00	50-60
Sikadur 300 epoxy	-	1.7	55	3.00	50-60
Sikadur 330 epoxy	-	3.8	30	1.50	50-60

3.1. Test setup and instrumentation

Beams and slabs were exposed to fire on their soffits and exposed to ambient temperature on their top surfaces. Slabs were tested in the intermediate-scale furnace at NRC and beams were tested in the full-scale floor furnace, also at NRC. These furnaces were designed to produce temperature and loading conditions as prescribed in ASTM E119 (2008) and CAN/ULC S101 (2007). No load was applied on the slabs except for their self weight. To record temperature variations in the specimens, 12 thermocouples were installed on each slab and 48 thermocouples on each beam. Electrical resistance strain gauges and fibre optic sensors were installed on the beams to capture strain and temperature during the tests (see Figure 1 and Figure 2).

Beams were loaded to their service load at room temperature and the load was kept constant for approximately 1 hour. Beams were exposed to fire immediately after the loading procedure was completed.

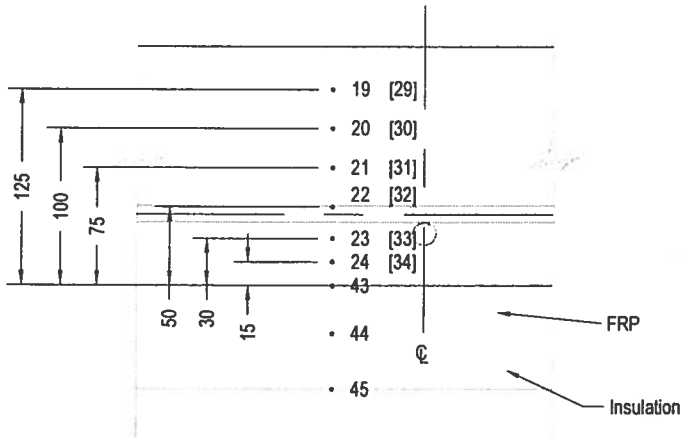

Figure 2. Location of thermocouples in slab dimensions in mm.

4. TESTS RESULTS AND DISCUSSION

4.1. Slabs

Minor shrinkage cracks were present on the insulation surface before the fire test and these cracks widened as the test progressed. Despite these cracks, no debonding of insulation occurred during the test. Figure 3 shows temperatures at the FRP-concrete bondline and at the locations of the steel reinforcement during the fire tests. These data indicate that it will be difficult to maintain the FRP temperature below the glass transition temperature (T_g) of the matrix for prolonged periods of time during fire. Temperatures in slab-B are lower compared to those in slab-A because of the thicker layer of insulation, but the FRP is still not kept below its T_g for the full duration of the fire. In both cases, the FRP-concrete temperature reaches T_g = 60 °C in aproximately 30 minutes. The average unexposed surface temperature after 4 hours of fire exposure reached 88 °C and 62 °C in slab A and B, respectively.

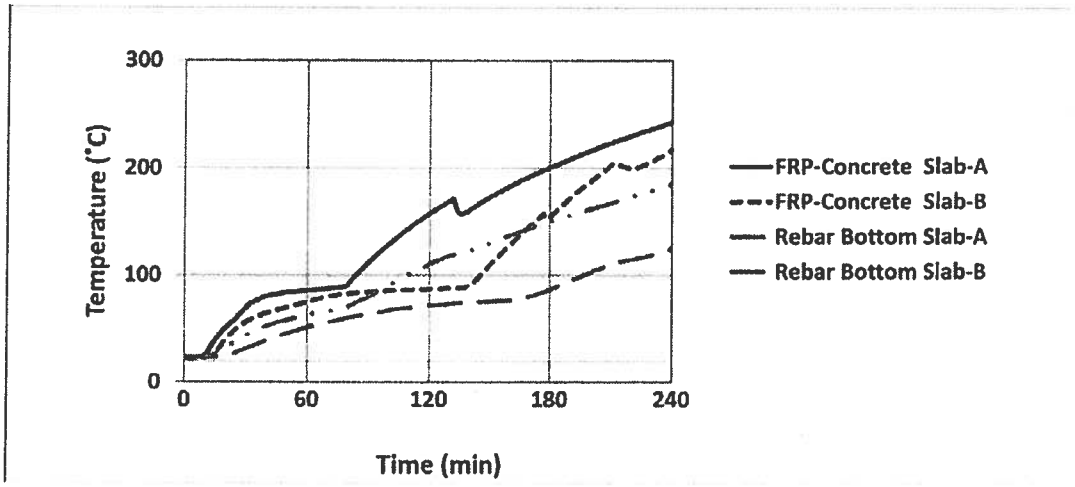

Figure 3. Temperature results for slabs (FRP-concrete bondline and steel reinforcement locations).

4.2. T-beams

Minor shrinkage cracks were also evident on the insulation surface of the T-beams before fire test and these cracks widened as the test progressed. After approximately one hour and 20 minutes, pooling and evaporation of water were visible on the unexposed surface. Shortly thereafter (approximately one hour and 30 minutes into the test), visible flame was observed coming out of cracks on the insulation. More flaming was evident near the U-wrap locations. After 4 hours of standard fire exposure, the beams did not fail, and therefore, the load was increased to the maximum capacity of the hydraulic system, but neither of the beams failed. Additionally, no spalling of insulation occurred during the tests. Figure 4 shows the temperature distribution at the insulation surface, the FRP-insulation interface, and the FRP-concrete interface (concrete surface) at midsection of the beams. The temperature at the FRP-concrete bondline reached T_g in approximately 30 minutes. For beam-A, a spike in the temperature on the surface of the FRP (location 2) occurred after approximately 30 minutes of fire exposure. The temperature increased to just over 400 °C and then decreased to just over 200 °C after 60 minutes of exposure. No similar spike in temperature was observed between the FRP and the concrete surface (location 3). Thus, the temperature spike was localized and was likely due to a crack in the insulation that widened initially but then closed slightly over time.

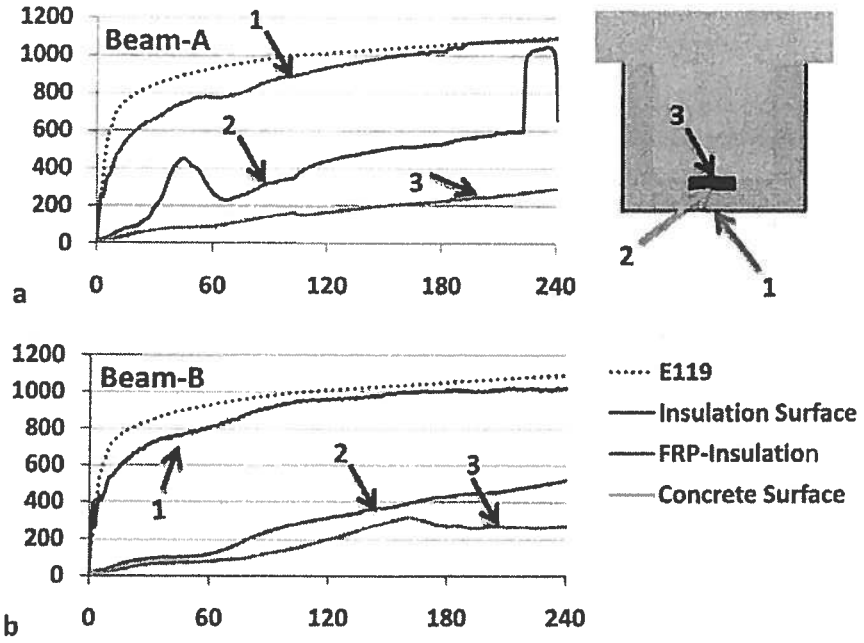

Figure 4. Temperature results for a) beam-A and b) beam-B (schematic drawing not to scale).

5. NUMERICAL HEAT TRANSFER MODEL

High temperatures cause severe damage to concrete, steel and FRP. Therefore, predicting the temperature distribution in a structural member is a crucial step in understanding the behaviour of the member. A major challenge is the simulation of the concrete due to its complicated chemical and structural composition. Portland cement paste may undergo various changes such as dehydration, porosity increase, thermal cracking, spalling and many others. Several models have been proposed for hygrothermo-mechanical simulation of concrete. Some existing models account for a coupled field heat and mass transfer problem. These models are capable of predicting temperature and pore pressure during exposure to elevated temperatures (Gawin et al., 1998, Mounajed and Obeid, 2004). If only temperatures are required, several simplifications can be made, which lead to the solution of a decoupled field equation. The following assumptions are usually made for decoupling the problem:

- Temperature of the fluid and the solid are the same at each point.
- The amount of heat transferred by mass diffusion is negligible.
- Evaporation of chemically and physically bound water is negligible (Capua, 2007).

Even more simplified methods for predicting temperature distribution in concrete sections which use a pre-determined temperature variation in the concrete section are available (Wickstrom, 1986, Malhotra, 1982). Although these methods provide a reasonable approximation in some problems, they are not suitable for complex geometries.

The model developed here is a finite-volume (FV) code that is capable of predicting temperature in an insulated concrete section. The partial differential equation of heat conduction can be expressed as

$$\rho c \frac{\partial T}{\partial t} = \nabla.(k \nabla T) = \frac{\partial}{\partial x}\left(k \frac{\partial T}{\partial x}\right) + \frac{\partial}{\partial y}\left(k \frac{\partial T}{\partial y}\right) \quad \text{Eq. 1}$$

where k is thermal conductivity, ρ is density, c is heat capacity, T is temperature, t is time, and x and y are spatial coordinates.

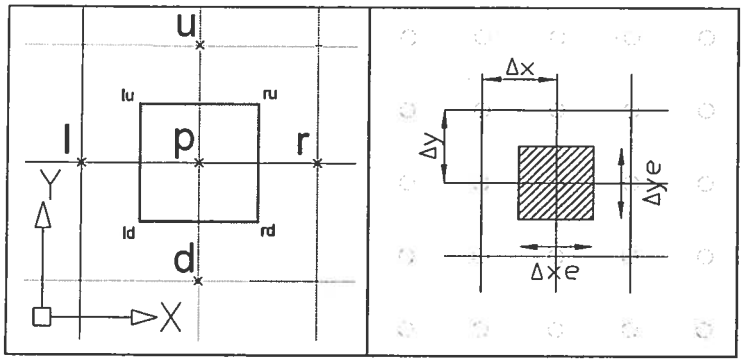

Figure 5. Spatial discretization.

For a two-dimensional rectangular grid, the discretized field equation is:

$$T_p^{i+1} = \left[a_*^0 T_p^i + a_d^0 T_d^i + a_l^0 T_l^i + a_r^0 T_r^i + a_u^0 T_u^i + b^0\right]/a_p^0 \qquad \text{Eq. 2}$$

where T_p^{i+1} is the temperature at point p at time step $t = t^{i+1}$. Other terms are described below:

$$a_*^0 = -\left(-a_p^0 + a_d^0 + a_l^0 + a_r^0 + a_u^0 + h_f^i \Delta L_r + h_c^i \Delta L_c\right) \qquad \text{Eq. 3}$$

$$b^0 = h_f^i T_f^i \Delta L_r + h_c^i T_c^i \Delta L_c \qquad \text{Eq. 4}$$

$$-a_p^0 = [\rho c]_p^i \frac{\Delta x_e \Delta y_e}{\Delta t} \qquad \text{Eq. 5}$$

$$a_d^0 = k_{pd}^i \frac{\Delta x_e}{\Delta y}, a_l^0 = k_{pl}^i \frac{\Delta y_e}{\Delta x}, a_r^0 = k_{pr}^i \frac{\Delta y_e}{\Delta x}, a_u^0 = k_{pu}^i \frac{\Delta x_e}{\Delta y} \qquad \text{Eq. 6}$$

$k_{pd} = \left(\frac{2k_p k_d}{k_p + k_d}\right)$ is for a uniform grid 0 and $h_f^i \Delta L_r$ and $h_c^i \Delta L_c$ are radiation and free convection terms. The effect of moisture in the simulation is taken into account by increasing the heat capacity of moist concrete.

5.1. Verification

The model is used to simulate a rectangular concrete section similar to the one used by Lie and Woollerton (1988); the column is subjected to the ASTM E119 standard fire from all four sides. The cross-sectional dimensions of the section are 305 by 305 mm. The model prediction is compared with measured temperatures in Figure 6. Three points, A, B, and C with concrete covers of 6, 63, and 152 mm, respectively, are selected for comparison. For point A (near the surface), the model predicts the experimental results with a maximum deviation of approximately 50 °C up to just over 400 °C. At that point, larger discrepancies are noted, but the predicted temperatures are higher than those measured in the test. For points B and C, the temperatures are underestimated at the early stages (below 100 °C) and then slightly overestimated afterwards. These discrepancies near 100 °C occur because the model does not account for moisture migration away from the heated surface.

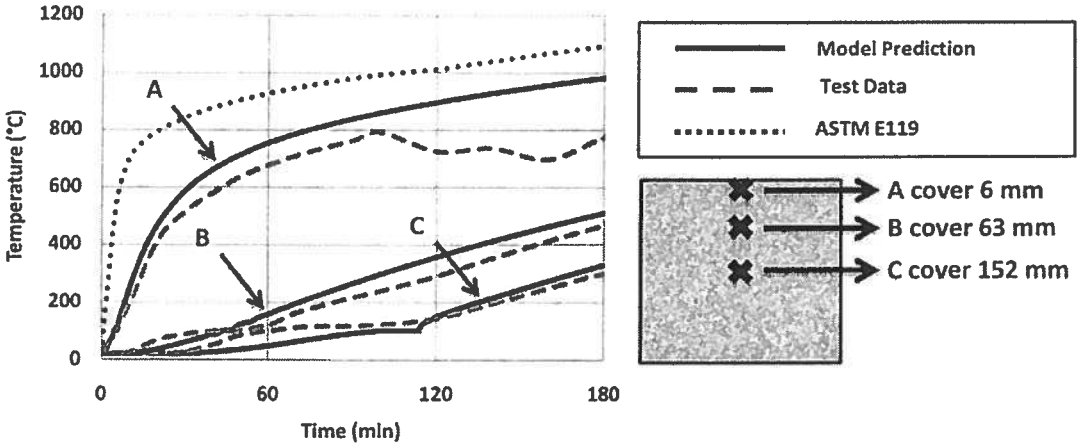

Figure 6. Predicted and measured temperatures as a function of exposure time for different depths within the concrete specimen (experimental data obtained from Lie and Woollerton, 1998).

5.2. Model results for slabs and T-beams

As shown in Table 1, two different insulation thicknesses were used in slab A and slab B. Figure 7 illustrates a comparison between model results and test data. Temperatures from the unexposed surface and FRP concrete interface are compared. The model predicts the temperature at the unexposed surface with a maximum discrepancy of 5 °C. For the temperature at the FRP concrete interface, the model prediction is not quite as close to the measurement. Once again the discrepancy occurs close to 100 °C and is related to the lack of modelling moisture migration. The maximum deviation between the prediction and the measured results is approximately 25 °C.

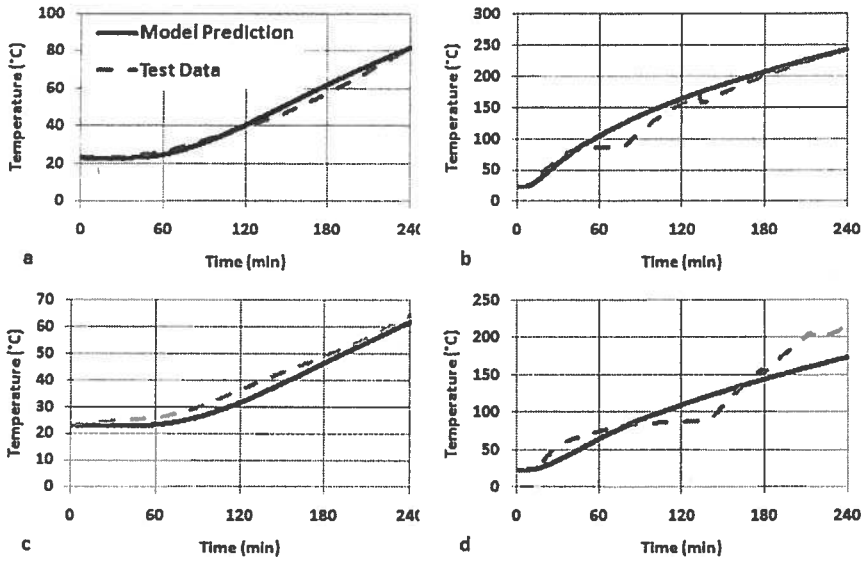

Figure 7. Predicted and measured temperatures as afunction of exposure time for slabs at, (a) unexposed surface slab-A (40 mm insulation thickness); (b) FRP-concrete interface slab-A; (c) unexposed surface slab-B and (d) FRP-concrete interface slab-B.

Figure 8 shows the temperature calculation from the model compared to temperatures measured in the fire tests for the T-beams. The dotted line is the average temperatures obtained from beam-A and beam-B. The model successfully predicts temperatures on the longitudinal steel and

FRP/concrete interface (with a maximum discrepancy of approximately 40 °C) which are crucial in predicting the structural behaviour of the strengthened member. The model is conservative in that it predicts higher temperatures than those measured in the tests.

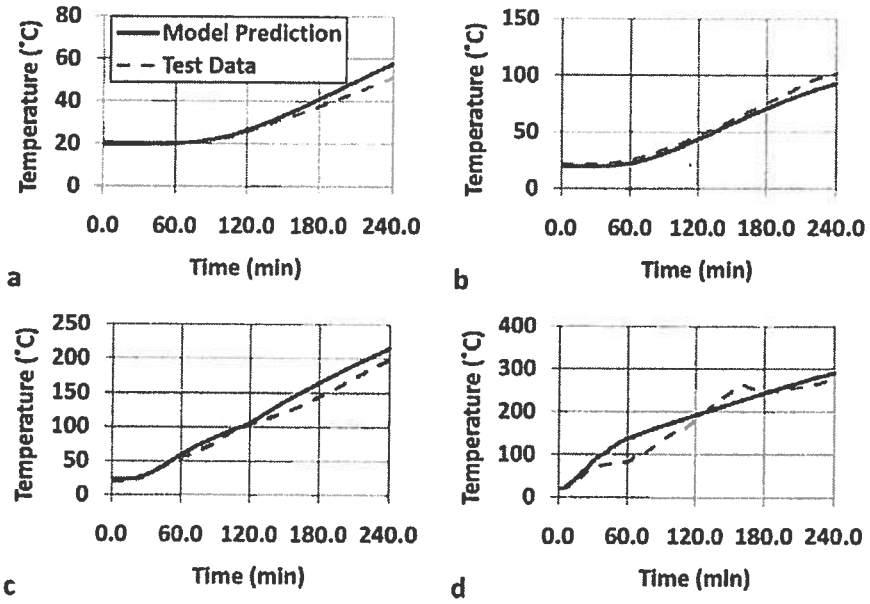

Figure 8. Predicted and measured temperatures vs. exposure time for T-beams at (a) unexposed surface; (b) on the centreline with concrete cover of 155 mm; (c) longitudinal steel and (d) FRP-concrete interface.

Although standard fire curves are widely used for determining the fire resistance of structural members, the intensity and duration of building fires may vary widely. Several parameters, such as amount of combustible material and ventilation, affect the severity and duration of compartment fires. In some cases, standard fire cures have serious deficiencies (Feasey and Buchanan, 2002). To investigate the effects of different time temperature curves on the response of T-beams, four different fire scenarios were selected. Fire time temperature curves were calculated using Equation 7, proposed by Lie (1992).

$$T_f = 250(10F)^{0.1/F^{0.3}} e^{-F^2 t}[3(1-e^{-0.6t}) - (1-e^{-3t}) + 4(1-e^{-12t})] + C\left(\frac{600}{F}\right)^{0.5} \quad \text{Eq. 7}$$

where T_f is fire temperature, t is time in hours and C is is a constant related to the boundary materials. Different fire loads (Q) and opening factors (F) for different fire scenarios are given in Table 4. Figure 9 shows the time temperature curves for Fires I to IV.

Table 4. Parameters used to produce fire curves.

	$F\ (\sqrt{m})$	$Q\ (kg/m2)$	C
Fire I	0.01	30	0.0
Fire II	0.05	30	0.0
Fire III	0.10	30	0.0
Fire IV	0.10	100	1.0

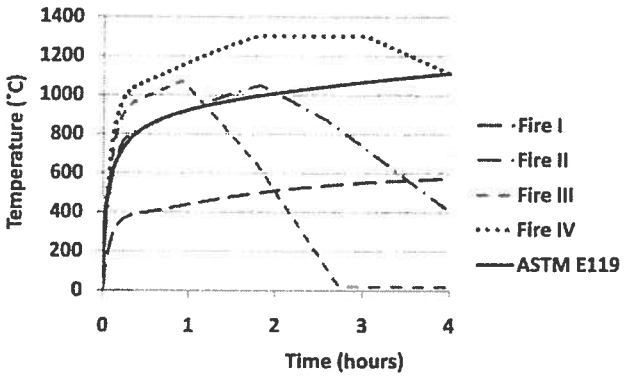

Figure 9. Time temperature curves for four different fire scenarios.

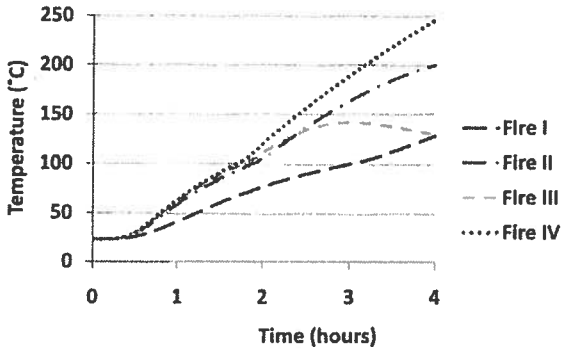

Figure 10. Longitudinal steel temperature for Fires I to IV.

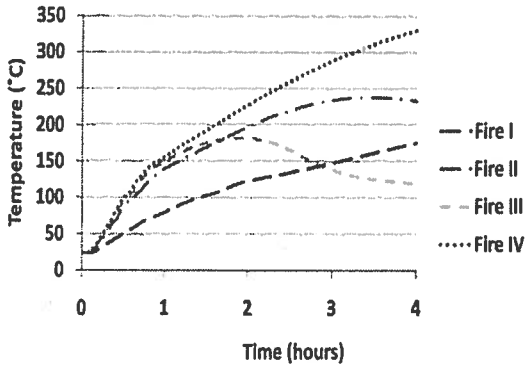

Figure 11. FRP-concrete interface temperature for Fires I to IV.

According to Figure 10, after four hours of exposure to fires I to IV, the longitudinal steel temperature in all scenarios remain below 250 °C. Under these scenarios, the steel retains most of its tensile strength after fire exposure (more than 90 percent). Given the fact that the temperature of the compression concrete (close to unexposed surface) is lower than the steel temperature, concrete will suffer even smaller losses in strength. As a result, the reduction in the moment capacity of the unstrengthened section will be minimal. While insulation provides limited protection for FRP in fire situations (less than 30 minutes, Figure 11), it plays a major role in protecting the reinforcing steel and concrete.

6. CONCLUSIONS

All specimens achieved a 4-hour fire endurance according to ASTM E119 specifications.

The insulation system effectively protected T-beams and slabs mainly by keeping internal steel temperatures below 250 °C.

The heat transfer model could successfully predict temperatures inside the section.

Results of numerical simulation using different fire scenarios predict that the T-beams will retain most of their unstrengthened room temperature strength regardless of the fire scenario.

7. ACKNOWLEDGEMENTS

The authors would like to thank the Intelligent Sensing for Innovative Structures (ISIS Canada) Research Network, the Natural Sciences and Engineering Research Council of Canada (NSERC) and Sika for the financial support of this project. The authors are also grateful to the technical staff in the Department of Civil Engineering, Queen's University and at the Fire Research Program, National Research Council of Canada.

8. REFERENCES

ACI. *Guide for the Design and Construction of Externally Bonded FRP Systems for Strengthening Concrete Structures,* American Concrete Institute, Farmington Hills, MI, 2008. ACI 440.2R-08.

ASTM. *Standard methods of fire test of building construction and materials*, American Society for Testing and Materials, West Conshohocken, PA, 2008. Test Method E119a -08.

Bazant, Z.P., Kaplan, M.F. *Concrete at high temperatures: material properties and mathematical models* Longman, London, 1996.

Blontrock, H., Taerwe, L., & Vandevelde, P. Fire Tests on Concrete Beams Strengthened with Fibre Composite Laminates. *Third PhD Symposium*, Vienna, Austria, 2000, 10 pp.

Buchanan, A.H., *Structural Design for Fire Safety*. Wiley, London, 2001.

Capua, D.D., and Mari, A.R. (2007). Nonlinear analysis of reinforced concrete cross-sections exposed to fire. *Fire Safety Journal* **42**, No. 2: 139-149.

Chowdhury, E.U, Eedson, R., Bisby, L.A., Green, M.F. & Benichou, N. (2009). Mechanical Characterization of Fibre FRP Materials at High Temperature. *Fire Technology.* Online 8 Nov 2009.

Deuring, M. *Brandversuche an Nachtraglich Verstarkten Tragern aus Beton*. Swiss Federal Laboratories for Materials Testing and Research, Dubendorf, Switzerland, 1994. Research Report EMPA No. 148,795.

Feasey, R. & Buchanan, A.H. (2002). Post-flashover fires for structural design. *Fire Safety Journal* **37**, No. 1: 83–105.

Gawin, D., Majorana, C., Pesavanto, F., & Schrefler, B. A fully coupling multiphase model of higro-thermo-mechanical behavior of concrete at high temperature. *Computational mechanics, new trends and applications.* Barcelona, Spain: CIMNE, 1998, 1–19.

Lie, T.T. *Structural Fire Protection.* American Society of Civil Engineers, New York, 1992, Manuals and Reports on Engineering Practice No. 78.

Lie, T.T., & Woollerton, J.L. Fire resistance of reinforced concrete columns, *Institute for Research in Construction, National Research Council of Canada*, Ottawa, Canada, 1988. Internal Report No. 569.

Malhotra, H.L. *Design of Fire-Resisting Structures*. Surrey University Press, London, 1982.

Mounajed, G. & Obeid, W. (2004). A new coupling F.E. model for the simulation of thermal hydro-mechanical behavior of concrete at high temperatures. *Materials and Structures* **37**, No. 6: 422–32.
Patankar, S.V. *Numerical heat transfer and fluid flow*, Hemisphere, New York, 1980.
Purkiss, J. A. *Fire Safety Engineering: Design of Structures*. Elsevier, Burlington, 2007.
ULC. *Standard Methods of Fire Endurance Tests of Building Construction and Materials* Underwriters Laboratories Canada, Toronto, Canada, 2007. CAN/ULC-S101-07
Wickstrom, U. A very simple method for estimating temperature in fire exposed concrete structures, Fire Technology Technical Report SP-RAPP 1986, 46, Swedish National Testing Institute, 1986, 186–194.
Williams, B.K., Kodur, V.K.R., Green, M.F., & Bisby, L.A. (2008). Fire Endurance of FRP Strengthened Concrete T-Beams. *ACI Structural Journal* **105**, No. 1: 60-67.